



## Effect of the Slope on the Bearing Capacity of a Strip Footing under Eccentric Loads

Salah Zerguine<sup>1\*</sup>, Samir Djireb<sup>2</sup> and Djamel Benmeddour<sup>1</sup>

<sup>1</sup>Department of Civil Engineering and Hydraulic, Mohamed Khider University, Biskra, Algeria

<sup>2</sup>Department of Civil Engineering and Hydraulic, Kasdi Merbah University, Ouargla, Algeria

\*Corresponding Author: Salah Zerguine, Department of Civil Engineering and Hydraulic, Mohamed Khider University, Biskra, Algeria

E-mail: sa\_zerguine@yahoo.fr, salah.zerguine@univ-biskra.dz

Received: January 28, 2019; Published: March 01, 2019

### Abstract

Agricultural areas have often characterized by the presence of slopes. The existence of buildings such as sheds, depots, mills, windmills in these areas is an obligation in a few times. The footings of these structures are generally subjected to eccentric vertical loads. This paper presents a numerical contribution of the analysis of strip footings subjected to eccentric loads near cohesionless slopes. The finite element software Plaxis 2D is used to estimate the effect of eccentric load on the bearing capacity. The results are illustrated using tables, graphs and failure envelopes. The obtained results are compared with those obtained by other researchers.

**Keywords:** Strip footings, eccentric loads, cohesionless slopes, finite element, bearing capacity, failure envelopes.

### Introduction

The estimation of the bearing capacity of a strip foundation based on a purely frictional soil, under the effect of eccentric and/or inclined loads is an important problem in the geotechnical field. The advanced method using failure envelopes in the corresponding loading plane. Two main methods are mentioned in the literature to predict the bearing capacity of foundations under eccentric and/or inclined loads: the classical method using correction factors and the advanced method using failure envelopes in the corresponding loading plane.

Several studies have been devoted for the calculation of the bearing capacity of shallow footings under eccentric and/or inclined loads on horizontal ground (Meyerhof [1], Butterfield and Gottardi [2], Musso and Ferlisi [3], Vulpe *et al.* [4], Rao *et al.* [5]). Other studies were done using the experimental method by means of laboratory model tests, Georgiadis and Butterfield [6], Okamura *et al.* [7], Ganesh *et al.* [8], Al-Zandi and Abbas. [9]

The case of a strip footing resting on the edge of a slope is a specific configuration, often encountered in practice. Many studies addressing this subject using analytical, empirical, and numerical methods are available (Saran and Reddy [10], Maréchal [11], Maloum and Sieffert [12], Krabbenhoft *et al.* [13], Turker *et al.* [14]. Zerguine *et al.* [15] estimated the bearing capacity using failure envelopes of eccentric vertical loads V-M, where they took into account the relative distance ( $d/B$ ) between the footing location

and the crest of slope forming an angle  $26.56^\circ$  with the horizontal. They showed that the eccentric vertical loading of a footing rested on the edge of a slope, causes a radical change of the shape of the failure envelopes. Also, they showed that the sign of eccentricity has a great effect on the distribution of normal stresses under a foundation placed on the crest of a slope.

Furthermore, for the special case of a strip footing behind a reinforced retaining wall, Zerguine *et al.* [16] investigated the bearing capacity using failure envelopes in the eccentrically vertical loading plane, for different parameters of wall geometry, reinforcement and soil properties. They have shown that the bearing capacity of the soil is not affected when the relative distance  $d/B$ , between the wall facing and the edge of the foundation is greater than or equal to 10.

In the present study, a series of numerical calculations, by means of finite-element code Plaxis [17], are carried out to estimate the bearing capacity of strip footings resting on a cohesionless slope and subjected to eccentric vertical loads. The results of this research are presented in the form of tables and curves, and they have compared with those available in the literature.

### Numerical method

In the present study, the software Plaxis based on finite-element was used to calculate the bearing capacity of a surface rough strip footings located on a cohesionless slope under eccentric loading.

The soil field was modelled of width 20 m and depth 7 m (Fig. 1-a), the soil domain was discretized as 15 node triangular elements. In order to test the influence of the mesh size, a series of numerical calculations have been performed. The mesh under the footing base and around the footing corners is refined in order to have smaller elements and graded mesh for which a more accurate solution was obtained. Both right and left vertical borders of the model were blocked horizontally, whereas the base was blocked in all directions. The boundary conditions and finite-element mesh for a surface strip footing resting at the crest of a cohesionless slope with height  $H = 3\text{ m}$  are shown in Figure 1-b. The method called "probe" loading technique is used in this study. The footing load is applied in increments up to failure under load eccentricity  $e/B$ , with respect to the reference point of pure vertical loading ( $e/B = 0$ ). Each analysis using probe method leads to determine a single failure load which is marked as a point in the failure envelope ( $V$ - $M$ ). All numerical analyses were performed for rough footings.

For the soil behavior, a linearly elastic-perfectly plastic Mohr Coulomb model is used and both associated and non-associated flow rule are adopted in this study. The following parameters are used: the Poisson ratio  $\nu = 0.3$ , the unit weight of the soil  $\gamma = 20\text{ kN/m}^3$  and the Young modulus  $E = 52\text{ MPa}$ , three angles of internal friction of soil are adopted  $\varphi = 25^\circ, 30^\circ$  and  $35^\circ$ . The footing was modelled as a weightless rigid plate element with an important Young's modulus and enough thickness.

**Presentation of the problem**

The bearing capacity of a strip footing located on a cohesionless slope under vertical eccentric load is given using the following equation based on Terzaghi's equation [18]:

$$q_u = \frac{1}{2} \gamma B N_\gamma i_{\gamma\beta} i_e \dots\dots (1)$$

where  $N_\gamma$  is the bearing capacity factor,  $i_e$  is a reduction factor representing the effect of eccentricity,  $i_{\gamma\beta}$  is a reduction factor defined by the following relation:

$$i_{\gamma\beta} = \frac{q_u(d/B, \beta)}{q_u(\beta=0)} \dots\dots (2)$$

Knowing that  $q_u(d/B, \beta)$  is the bearing capacity of a strip footing located on a slope, and  $q_u(\beta=0)$  is the bearing capacity of a strip footing located on level ground.

In the case of strip footings located on sand slope under eccentric and/or inclined loads, Ganesh *et al.* [8] recommended a reduction factor RF, that takes into account both eccentric and inclined loads, and the depth of footing, this factor is given by as follows:

$$RF = \left[ \left( 1 - \frac{2e}{B} \right) \left( 1 - \frac{\alpha}{\varphi} \right) \right]^n \dots\dots (3)$$

Where  $n = 2$  for the case  $D/B = 0$ , knowing that  $D$  and  $B$  are the depth and the width of footing successively,  $e$  is the vertical eccentric load,  $\alpha$  is the load inclination angle and  $\varphi$  is the internal friction angle of soil.

Gottardi and Butterfield [19] noted that the failure surface for a strip footing located on horizontal ground can be characterized by a second-order equation as follows:

$$\frac{M}{BV_{\max}} = 0.36 \frac{V}{V_{\max}} \left( 1 - \frac{V}{V_{\max}} \right) \dots\dots (4)$$

Where  $V_{\max}$  is the ultimate vertical load,  $V$  is the vertical collapse load corresponding to the eccentricity of the vertical load, and  $M$  is the moment at foundation level.

The objective of the present study is to determine the bearing capacity of soil near a cohesionless slope, for different load eccentricities  $e/B$ , taking account several parameters such as angle of slope, angle of internal friction and angle of dilation. The geometry and loading conditions are illustrated in Figure 1.

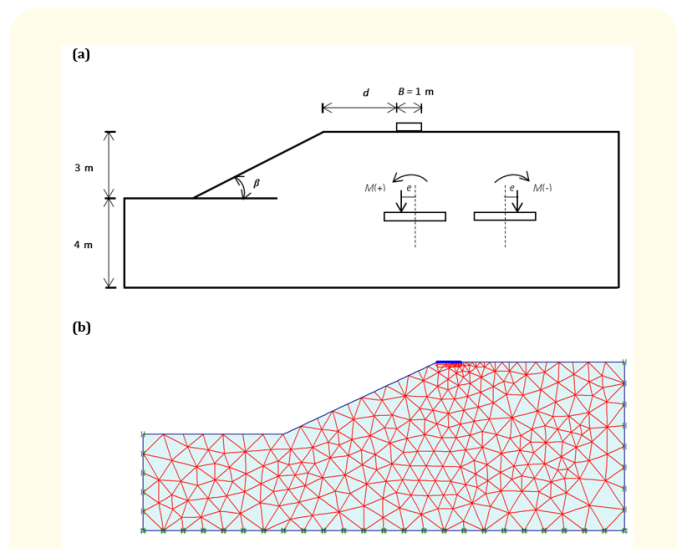


**Figure 1:** Presentation of the problem studied: (a) geometry of the slope; and (b) undeformed mesh.

A strip footing of width  $B = 1\text{ m}$  is located at a distance  $d$  from the crest of a slope with height  $H = 3\text{ m}$  and slope angle  $\beta = 15^\circ, 20^\circ, 25^\circ$  and  $30^\circ$ . The applied eccentric load can be positive or negative (Fig. 1-a). For  $\beta = 25^\circ$ , different relative footing distances from the crest of the slope  $d/B = 0, 1, 2$  and  $3$  were considered for  $\varphi = 30^\circ$ . However, for slopes with  $\beta = 15^\circ, 20^\circ$ , and  $30^\circ$ , the foundation is considered placed only on the crest of the slope. Three values of internal friction angle of soil are considered in this study,  $\varphi = 25^\circ, 30^\circ$  and  $35^\circ$ .

Results and Discussion

Strip footing located on horizontal ground ( $\beta = 0$ )

The failure envelope characterizes the surface that governed the collapse of the soil under the foundation. All points in the failure envelope are determined using the "probe" test analysis. Failure envelopes (V-M) in plane, for a strip footing under eccentric loads and located on horizontal ground, are presented in Figure 2.

The obtained results are compared with those estimated by the equation proposed by Gottardi and Butterfield [19] and the others obtained by Meyerhof's approach [1]. It is noticed that the failure envelopes have a parabolic shape where the maximum value  $M = 0.081 BV_{max}$  occurring for  $V/V_{max} = 0.54$ . The numerical results of this study present a good agreement with those given by Gottardi and Butterfield [19], excepting for great values of  $M/BV_{max}$  that overestimate the present results of this study. However, the present solution overestimates the results given by Meyerhof [1]. The limit load calculated corresponding to horizontal level for  $\varphi = 30^\circ$  is equal to 168 KN/m.

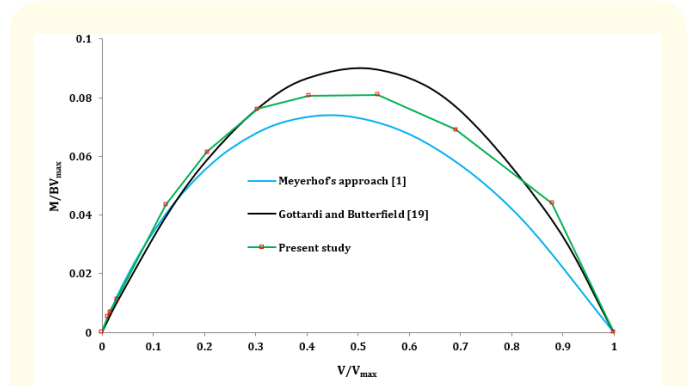


Figure 2: Failure envelopes (V-M) plane estimated by several approaches, with a friction angle  $\varphi = 30^\circ$ .

Tables 1 to 4 summarize the limit loads of a strip foundation rested on the crest of slope at different angles of inclination. Generally, it is remarkable that limit loads increase with increasing of both internal friction angle  $\varphi$  and dilation angle  $\psi$ . Wireless, limit loads decrease with increasing of the slope angle  $\beta$ .

Table 1: Limit loads values for slope angle:  $\beta = 15^\circ$

$\varphi$ $e/B \backslash \psi$	$\varphi = 25^\circ$			$\varphi = 30^\circ$			$\varphi = 35^\circ$		
	$\psi = \varphi$	$\psi = \varphi/2$	$\psi = 0$	$\psi = \varphi$	$\psi = \varphi/2$	$\psi = 0$	$\psi = \varphi$	$\psi = \varphi/2$	$\psi = 0$
-0.5	4.55	4.63	5.11	3.01	5.25	4.47	6.41	5.94	4.49
-0.4	8.24	9.74	8.68	8.01	15.07	14.13	12.03	27.57	16.47
-0.3	20.97	18.60	17.30	12.74	37.78	32.54	17.15	70.71	43.6
-0.2	35.20	33.58	30.29	48.24	69.66	56.02	26.78	136.84	105.01
-0.1	51.32	49.51	45.31	77.05	101.96	82.71	49.36	217.73	150.12
0	53.02	52.37	48.51	108	105.06	90.37	225.86	216.07	169.24
0.1	37.22	36.66	33.53	90	75.55	65.47	161.94	156.96	123.2
0.2	23.66	23.18	21.15	72.45	46.86	41.25	100.76	97.91	76.51
0.3	10.66	12.39	12.49	41.46	21.3	21.77	20.57	36.92	37.25
0.4	5.30	6.40	5.92	11.79	7.20	8.68	15.50	11.01	8.74
0.5	2.87	3.13	2.87	5.02	3.10	3.43	5.40	4.50	3.13

Table 2: Limit loads values for slope angle:  $\beta = 20^\circ$

$\varphi$ $e/B \backslash \psi$	$\varphi = 25^\circ$			$\varphi = 30^\circ$			$\varphi = 35^\circ$		
	$\psi = \varphi$	$\psi = \varphi/2$	$\psi = 0$	$\psi = \varphi$	$\psi = \varphi/2$	$\psi = 0$	$\psi = \varphi$	$\psi = \varphi/2$	$\psi = 0$
-0.5	4.46	4.58	4.52	5.14	5.22	5.07	6.46	5.51	5.82
-0.4	8.99	8.97	7.51	12.07	14.49	11.83	16.54	21.74	15.30
-0.3	13.40	19.63	17.61	20.30	37.49	31.69	31.25	70.29	41.16
-0.2	22.17	29.64	26.83	63.24	59.06	50.39	47.38	122.19	89.87
-0.1	40.71	39.01	34.25	87.25	82.58	65.24	183.14	171.12	124.4
0	36.65	35.80	32.66	77.87	75.47	65.11	129.94	159.81	124.27
0.1	25.75	25.19	23.17	48.91	52.19	45.69	113.75	110	74.64
0.2	16.82	16.41	14.96	34.16	32.91	29.35	68.97	66.10	42.49
0.3	8.17	9.68	9.13	17.18	17.09	15.60	15.68	27.38	21.13
0.4	4.79	4.81	4.29	6.83	6.40	5.76	7.57	7.80	7.58
0.5	2.85	2.66	2.58	3.24	2.89	2.63	3.54	3.41	3.46

**Table 3:** Limit loads values for slope angle:  $\beta = 25^\circ$

$\varphi$	$\varphi = 25^\circ$			$\varphi = 30^\circ$			$\varphi = 35^\circ$		
$\psi$ e/B	$\psi = \varphi$	$\psi = \varphi/2$	$\psi = 0$	$\psi = \varphi$	$\psi = \varphi/2$	$\psi = 0$	$\psi = \varphi$	$\psi = \varphi/2$	$\psi = 0$
-0.5	3.64	3.29	3.13	4.30	2.77	2.70	4.23	3.94	3.81
-0.4	5.83	7.96	7.11	15.8	9.33	8.22	12.17	15.27	14.90
-0.3	16.33	15.86	14.16	27.06	23.92	20.25	27.43	60.19	32.19
-0.2	21.78	20.96	18.19	39.51	35.03	26.89	28.25	95.72	63.58
-0.1	25.58	24.50	21.44	46.88	44.20	35.03	129.16	122.12	91.37
0	22.50	21.97	19.54	40.16	39.31	34.09	109.62	112.77	90.26
0.1	15.98	15.62	14	27.57	27.22	24.06	80.95	77.50	63.02
0.2	10.63	10.34	9.05	16.22	17.13	14.87	49.40	46.31	38.79
0.3	6.64	6.31	6.11	7.19	8.85	8.67	11.74	17.93	18.38
0.4	3.52	3.33	3.40	4.11	2.97	3.58	6.33	5.83	4.50
0.5	2.63	4.24	3.66	1.95	1.92	1.71	2.89	2.69	2.39

**Table 4:** Limit loads values for slope angle:  $\beta = 30^\circ$

$\varphi$	$\varphi = 25^\circ$			$\varphi = 30^\circ$			$\varphi = 35^\circ$		
$\psi$ e/B	$\psi = \varphi$	$\psi = \varphi/2$	$\psi = 0$	$\psi = \varphi$	$\psi = \varphi/2$	$\psi = 0$	$\psi = \varphi$	$\psi = \varphi/2$	$\psi = 0$
-0.5	collapse of the slope			4.51	4.31	3.71	4.01	4.01	3.86
-0.4	collapse of the slope			11.62	15.63	13.87	31.69	20.02	15.23
-0.3	collapse of the slope			26.22	24.55	20.40	57.20	52.25	33.52
-0.2	collapse of the slope			33.59	30.47	23.83	80.09	71.35	51.77
-0.1	collapse of the slope			38.32	34.54	25.05	94.14	86.27	66.96
0	collapse of the slope			32.74	31.22	22.90	80.15	73.88	59.95
0.1	collapse of the slope			23.10	21.99	16.96	56.52	53.31	39.61
0.2	collapse of the slope			15.09	14.53	12.61	34.95	33.16	27.20
0.3	collapse of the slope			7.81	8.29	8.01	10.69	16.17	15.18
0.4	collapse of the slope			4.01	4.85	3.81	5.93	5.79	3.70
0.5	collapse of the slope			2.24	2.28	2.27	2.27	2.80	2.24

**Effect of slope angle ( $\beta$ )**

Figure 3 shows the bearing capacity of a strip footing resting on the edge of slope for several values of slope inclination angle  $\beta$ . It is noticed that the increasing slope angle causes a diminution in bearing capacity. The decrease of the bearing capacity becomes very important if the angle of slope  $\beta$  is equal or exceeds the value  $25^\circ$ . The limit load applied to the foundation is centric for the case of a slope inclined by an angle  $\beta = 15^\circ$ . However, for an angle  $\beta \geq 20^\circ$ , all limit loads are eccentric by  $e/B = -0.1$ . On the other hand, negative eccentricities lead to higher limit loads than those due to positive eccentricities.

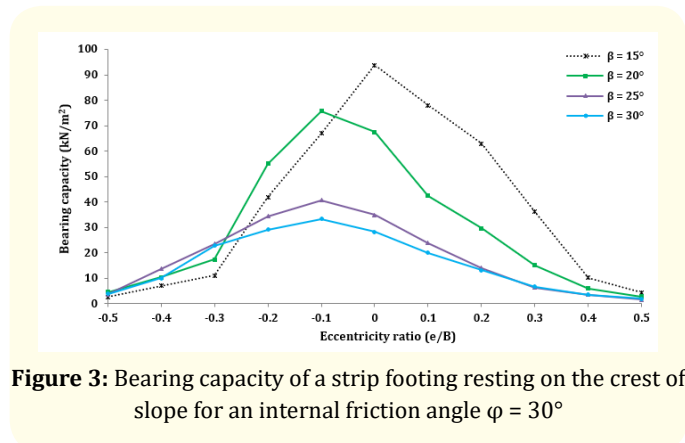


**Figure 3:** Bearing capacity of a strip footing resting on the crest of slope for an internal friction angle  $\varphi = 30^\circ$

**Effect of dilatant angle  $\psi$**

Figure 4 shows the bearing capacity as function of eccentricities for the internal friction angle  $\varphi = 25^\circ$  with varied values of the dilatation angle:  $\psi = \varphi, \varphi/2$  and 0. It is known that the bearing capacity of the soil increases by decreasing the dilatation angle. The angles  $\beta \geq 25^\circ$  cause a considerable decrease in the bearing capacity of the soil. Also, the limit load in cases  $\beta = 20^\circ, 25^\circ$  and  $30^\circ$  is eccentric by  $e = -0.1 B$ , where this load becomes centric in the case of a slope with an angle  $\beta \leq 15^\circ$ . Moreover, the negative eccentricity causes larger limit loads than those induced by the positive eccentricity.

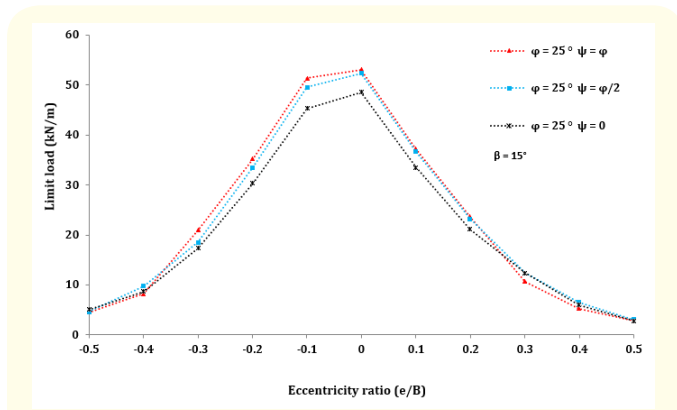


**Figure 4:** Effect of dilatation angle on the bearing capacity of a strip footing located on the crest of slope with  $\beta = 15^\circ$  and  $\varphi = 25^\circ$

**Effect of friction angle  $\varphi$**

Figure 5 shows the bearing capacity as function of eccentricities for an associated flow rule, taking into account different angles of dilatation  $\psi = \varphi, \varphi/2$  and 0. It is known that the bearing capacity of

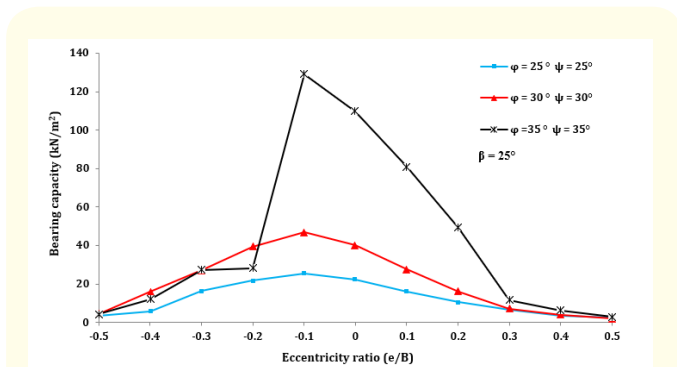


**Figure 5:** Effect of internal friction angle on the bearing capacity of a strip footing located on the crest of slope with  $\beta = 25^\circ$

the soil increases by decreasing the friction angle. The difference between the limit loads corresponding to the angles  $30^\circ$  and  $35^\circ$  is significant. However, the negative eccentricity causes decreasing of the bearing capacity because of the collapse mechanism witch developed at the edge of the slope for higher internal friction angles.

**Effect of slope on the shape and size of failure envelopes**

Figure 6 shows the normalized failure envelopes (V-M) obtained from the numerical analyses, for a strip footing located on the edge of a cohesionless slope with different angles  $\beta = 15^\circ, 20^\circ, 25^\circ$  and  $30^\circ$  with  $\varphi = 30^\circ$ .

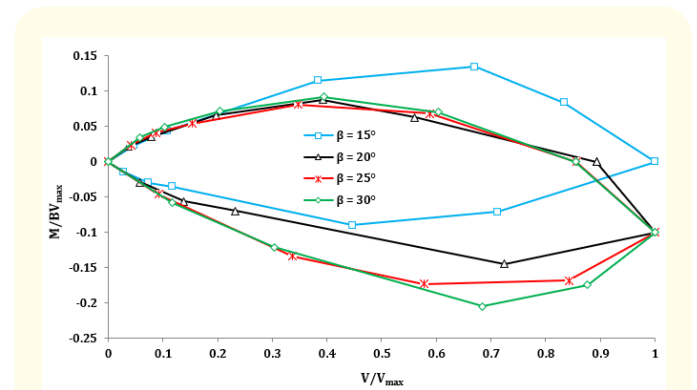


**Figure 6:** Failure envelopes (V-M) in plane estimated for different values of the slope angle, with an internal friction angle  $\varphi = 30^\circ$ .

It is seen that the increase in the angle  $\beta$  leads to enlargement of the size of the failure envelopes of the negative side of the moments. For an angle  $\beta \geq 20^\circ$ , all the curves turn around the origin of the center (0,0) in the direction of the clockwise.

**Effect of the relative distance on the bearing capacity**

Figure 7 shows the bearing capacity of a strip footing resting near a slope inclined by an angle  $\beta = 25^\circ$ , with an angle of friction  $\beta = 30^\circ$ , calculated for different relative distances  $d/B$  from the crest of slope. It is seen that the bearing capacity increases by increasing the distance between the crest of slope and the edge of foundation. The eccentricity of the load causes the reduction of the bearing capacity. It is noticed that the increase in  $d/B$  leads to increasing the bearing capacity. This occurs in reason that the influence of slope on the bearing capacity disappears at a certain distance of the footing from the edge of the slope ( $d/B = 3$ ). The maximum value reached of the bearing capacity is  $168 \text{ kN/m}^2$ .

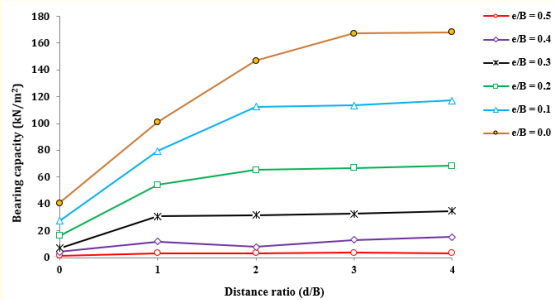


Figure 7: Bearing capacity as function of relative distance, with an internal friction angle  $\varphi = 30^\circ$ .

## Conclusion

The code Plaxis based on finite element analysis was used to estimate the limit loads for strip footings near a cohesionless slope. The footings is subjected to vertical eccentric loads. Several friction angles;  $\varphi = 25^\circ, 30^\circ$  and  $35^\circ$ ; dilation angles  $\psi = \varphi, \psi = 1/2\varphi$  and  $\psi = 0$ ; slope angles;  $\beta = 15^\circ, 20^\circ, 25^\circ$  and  $30^\circ$  are considered in this study. Different distances between the crest of the slope and the location of the foundation are taken into account. The obtained results are given in terms of tables, graphs and compared with other results available in the literature.

For the frequent case of a strip footing located on level ground, the present results are bracketed between the results of Gottardi and Butterfield [19] and those of Meyerhof's approach [1]. The Plotted failure envelopes are practically symmetrical for both negative and positive moment loading cases.

For the case of a strip footing located on the crest of a slope, several considerations are taken into account, such as internal friction angle, dilation angle and slope angle. In general, increasing values of an internal friction and dilation angles cause augmentation in value of bearing capacity, except of high values  $\varphi = \psi = 35^\circ$ , in the case of positive eccentricity. In other hand, increasing values of slope angle causes a diminution in bearing capacity especially for angles  $\beta \geq 25^\circ$  and produces a radical change in shape and size of the failure envelopes for the eccentric vertical loadings.

## Bibliography

- Meyerhof GGT. "The bearing capacity of foundations under eccentric and inclined loads". Proceedings of 3rd International Conference on SMFE 1.1 (1953): 440-445.
- Butterfield R and G Gottardi. "A complete three-dimensional failure envelope for shallow footings on sand". *Géotechnique* 44.1 (1994): 181-184.
- Musso Antonino and Settimio Ferlisi. "Collapse of a model strip footing on dense sand under vertical eccentric loads". *Geotechnical and Geological Engineering* 27.2 (2009): 265-279.
- Vulpe C., et al. "A generalised failure envelope for undrained capacity of circular shallow foundations under general loading". *Géotechnique Letters* 4.3 (2014): 187-196.
- Rao Pingping., et al. "Bearing capacity of strip footings on two-layered clay under combined loading". *Computers and Geotechnics* 69 (2015): 210-218.
- Georgiadis M and R Butterfield. "Displacements of footings on sand under eccentric and inclined loads". *Canadian Geotechnical Journal* 25.2 (1988): 199-212.
- Okamura Mits., et al. "Effects of footing size and aspect ratio on the bearing capacity of sand subjected to eccentric loading". *Soils and Foundations* 42.4 (2002): 43-56.
- Ganesh R., et al. "Bearing capacity of shallow strip foundations in sand under eccentric and oblique loads". *International Journal of Geomechanics* 17.4 (2016): 06016028.
- Al-Zandi., et al. "Experimental Study of a Strip Footing under Inclined and Eccentric Load on Geogrid Reinforced Sandy Soil". *Tikrit Journal of Engineering Sciences* 24.1 (2017): 70-80.
- Saran S and BS Reddy. "Bearing capacity of eccentrically loaded footings adjacent to cohesionless slopes". *Indian Geotechnical Journal* 20.2 (1990): 119-142.
- Maréchal Olivier. "Portance de fondations superficielles établies à proximité de talus et soumises à des charges inclinées et excentrées". *Diss. Nantes* (1999).
- Maloum S and J-G. Sieffert. "Interaction sol-fondation superficielle au voisinage de la crête d'un talus: analyse de la capacité portante". *Revue française de géotechnique* 100 (2002): 83-89.
- Krabbenhoft Sven., et al. "Lower-bound calculations of the bearing capacity of eccentrically loaded footings in cohesionless soil". *Canadian Geotechnical Journal* 49.3 (2012): 298-310.
- Turker Emel., et al. "Bearing capacity of eccentrically loaded strip footings close to geotextile-reinforced sand slope". *Canadian Geotechnical Journal* 51.8 (2014): 884-895.
- Zerguine Salah., et al. "Bearing capacity of eccentrically loaded strip footings near a slope". *Global Civil Engineering Conference*. Springer, Singapore (2017): 1285-1293.
- Zerguine Salah., et al. "Bearing capacity of a strip footing on a geosynthetic reinforced soil modular block walls after a seismic loading". *Journal of Applied Engineering Science and Technology* 4.1 (2018): 69-75.

17. Brinkgreve RBJ., *et al.* "Plaxis 3D 2012". Plaxis bv (2012).
18. Terzaghi Karl. "Theoretical soil mechanics". New York, Wiley, (1943).
19. Gottardi Guido and Roy Butterfield. "On the bearing capacity of surface footings on sand under general planar loads". *Soils and Foundations* 33.3 (1993): 68-79.

**Volume 3 Issue 4 April 2019**

**© All rights are reserved by Salah Zerguine., *et al.***